Electrochimica Acta 565 (2026) 148788

Contents lists available at ScienceDirect

Electrochimica Acta

journal homepage: www.journals.elsevier.com/electrochimica-acta

Rational design of sulfone-based electrolytes for dual-ion batteries

Mikhail V. Gorbunov [a,b,*], Cansin Bulut [a], Daria Mikhailova [a,b]

[a] Leibniz Institute for Solid State and Materials Research Dresden (IFW Dresden), Helmholtzstraße 20, 01069 Dresden, Germany
[b] Karlsruhe Institute of Technology, Institute for Applied Materials – Energy Storage Systems (IAM-ESS), Hermann-von-Helmholtz-Platz 1, 76344 Eggenstein-Leopoldshafen, Germany

ARTICLE INFO

Keywords:
Dual-ion batteries
Anionic intercalation
Sulfone-based electrolytes
Rational design
Salts synergy

ABSTRACT

Dual-ion batteries (DIB) with a graphitic cathode represent an intriguing concept, which remains challenging to commercialise. One of the key obstacles is selection of an electrolyte with a sufficiently broad window of electrochemical stability ($0\ V \leq E \leq 5.5$ V vs. Li^+/Li). Often, modern studies suggest either use of super-concentrated electrolytes ($C_M \geq 3$ M) or chemical modification of the solvent to walk round this problem. These approaches, however, result in decreased power density, a narrowed operating temperature window and increased cost of the final battery system.

Another option is to avoid using the super-concentration concept by selecting an appropriate combination of an electrochemically stable solvent and a combination of salts. This was realised in our work. We re-considered sulfones, known for their exceptionally high oxidative stability, as electrolyte solvents. Their instability within the anodic range of electrochemical potentials was tackled by mixing LiFSI and $LiPF_6$ salts. This resulted into following synergy: the presence of FSI^- anions ensured electrolyte compatibility with metallic lithium and graphite, serving as anodes, while a sufficient concentration of PF_6^- anions reduced the impact of current collector corrosion. Before long-term electrochemical tests, we conducted a preliminary physicochemical characterisation of a series of sulfone-based electrolytes, which can serve as a method for their rational development. Particular attention was paid to the impact of preparation and testing protocols onto long-term cycling behaviour. Besides, fundamental ways of improving the sulfone-based electrolytes were discussed. Ultimately, the most promising electrolyte-candidate was selected based on performance, sustainability, and price.

1. Introduction

Green agenda keeps the demand for secondary batteries high. Modern market of energy solutions for portable electronic devices is dominated by lithium-ion batteries (LIB) [1]. Within the recent years, they have also been introduced into the industry of electric vehicles, which raised the questions regarding the sufficiency of lithium supplies in the Earth's crust [2]. Although plenty of alternatives, including batteries based on the electrochemical (de)intercalation of different alkali- (Na, K), alkali-earth (Mg, Ca) and other metal-ions (Zn, Al, etc.) [2–7] into suitable host structures, have also undergone significant development over the last decade, they still have space for improvement. Mostly, they are considered for applications in large-scale electrochemical energy storage facilities, since there, the specific characteristics (such as charge and energy density) are a less critical requirement [2].

Another important problem that remains to be addressed, is improvement of already existing LIBs in terms of materials costs, eco-friendliness, energy efficiency, life cycle and recyclability. This can be attributed to the widely used term "sustainability" [8]. One of urgent goals here is to find a resource-efficient procedure of recycling, since a typical state-of-the-art lithium battery contains a mixture of elements that can be difficult to separate. Specifically, this relates to positive electrodes based on $LiCoO_2$, $LiFePO_4$ (LFP) or $Li_x(Ni, Mn, Co)O_2$ (NMC). Thus, industrial recycling of spent LIB is currently a rather complicated process [9].

In late 1980s, a concept was introduced, which could allow to circumvent the named issue. It is dual-graphite (dual-carbon), or more generally, dual-ion battery (DIB) [10]. The principle is based on the amphoteric properties of graphite, allowing it to form both cationic (acceptor-type) and anionic (donor-type) intercalation compounds. During charge of a DIB, anionic electrochemical intercalation occurs on the positive electrode, and cationic intercalation on the negative electrode, both made out of carbon [11]. Besides significant decrease in the

* Corresponding author.
E-mail address: mikhail.gorbunov@kit.edu (M.V. Gorbunov).

https://doi.org/10.1016/j.electacta.2026.148788
Received 20 January 2026; Received in revised form 31 March 2026; Accepted 31 March 2026
Available online 1 April 2026

price of the cathode materials, recycling of such systems is expected to be less sophisticated, as it would only require separation of graphite (carbon) from the electrolyte and binder. Numerous advances in this field have already been reported [12].

Despite their attractiveness, several fundamental obstacles exist, which severely hinder the practical application of DIB nowadays. First and foremost, it is the electrochemical potential of anionic intercalation. For example, PF_6^- anions intercalate at voltages well above 4.5 V vs. Li^+/Li, and a significant part of the process occurs above 5.0 V, if we consider room temperature (298 K) and electrolyte concentration $\leq$2 mol•kg^{-1} [11,13]. State-of-the-art carbonate-ester-based electrolytes are incapable of sustaining the oxidative decomposition at such high potentials. The most common approach of overcoming this issue is usage of super-concentrated electrolytes [14]. According to the well-known Nernst equation, electrochemical potential E of the anionic intercalation should reduce, if the activity of reduced species (PF_6^- or other anions) a_{red} increases:

$$E = E_0 + \frac{RT}{nF}\ln\frac{\Pi a_{iox}^{\nu_i}}{\Pi a_{jred}^{\nu_j}}. \quad (1)$$

The value of a_{red} grows along with the salt concentration. Thus, it was shown that the upper voltage cut-off of the *graphite|4 M LiPF$_6$/DMC|Li* cell can be limited by 5 V (DMC – dimethyl carbonate) [15]. However, it leads to a decrease of the system's specific power density. Further, compatibility of this electrolyte with a graphitic anode has not been studied. A few recent reports claim that well-operating dual-graphite battery cells can be made using the idea of super-concentrated electrolytes, and such cells are able to deliver hundreds of cycles with a decent capacity retention [16,17]. In spite of such possibilities, super-concentrated electrolytes (salt concentration $C \geq 3$ M) have two following disadvantages. These are price, which grows with the amount of lithium salt used [18], and the temperature range of operation, since often, such electrolyte systems are prepared on the verge of solubility limits for the corresponding salts [19]. If the temperature is slightly reduced, part of the salt should settle on the electrodes' surfaces or in between fibres of the separator, causing a drastic decrease of the battery performance. The mentioned issues should seriously limit the practical applicability of such electrolytes.

Along with the pivotal physical characterisation of the electrochemical PF_6^- anions' intercalation into graphite, an alternative electrolyte for dual-ion batteries was proposed in work [11], with ethyl methyl sulfone (EMS) serving as a solvent. It is possible to dissolve significant amount of various lithium salts in various sulfones, formulating electrolytes with acceptable electrical conductivity [20]. Generally, sulfones are known for their exceptionally high stability against electrochemical oxidation at high voltages [21]. In particular, EMS and tetramethylene sulfone, or sulfolane (TMS, SL), can be stable above 5.5 V vs. metallic lithium (depending on various parameters) [21,22], which makes them well-applicable for fundamental studies of electrochemical anionic intercalation. However, sulfones with simple hydrocarbon radicals are incompatible with the graphitic anode, most likely due to instability of the –SO_2– group against reduction at low electrochemical potentials [23]. In the literature, various strategies of overcoming this disadvantage have been proposed [24–26]. One of the most recent reports demonstrates a rather interesting approach of chemical modification of EMS to induce the electron delocalisation through enhanced resonance and electron-withdrawing effect. This was achieved by fluorination of the ethyl radical [24]. Other possibilities are represented by the concepts of localised high-concentration electrolytes [25], use of SEI-forming additives or use of selected co-solvents [26]. Chemical modification of the solvent should significantly increase the final battery price, whereas the other two options were not tested for the electrochemical stability above 5.0 V vs. Li^+/Li. Thus, being attractive either from the fundamental point of view, or for targeting the application of sulfone-based electrolytes with state-of-the-art high voltage cathodes like NMC, the use of the above approaches for DIB operating at extreme voltages might be limited, especially if the electrolyte concentration is reduced.

Another way of overcoming the problem of sulfones being unstable at low electrochemical potentials is to choose the right salt. To be more specific, some of the electrolyte salts are capable of forming a robust solid electrolyte interface (SEI) from the products of their decomposition. Typical examples are LiTFSI (lithium bis(trifluoromethanesulfonyl) imide) and LiFSI (lithium bis(fluorosulfonyl)imide [27]. Generally, this should mean more flexibility in selecting the electrolyte solvent, since if the salt forms the SEI itself, the reduction of the solvent at low potentials is inhibited. Moreover, solubility of lithium and other alkali metals' salts containing bis(sulfonyl)imide anions in different battery-relevant polar aprotic solvents is rather high, which opens the opportunity of developing super-concentrated sulfone-based electrolytes for dual-graphite batteries [28]. In this case, however, disadvantages of the super-concentrated electrolytes related to their price and operational temperature range remain. On the other hand, the use of super-concentration concept allows to reduce the impact of the main drawback of FSI^- and $TFSI^-$ anionic species. It is known, that FSI^- anions exhibit rather high corrosive activity against aluminium, which is a common cathode current collector material, at electrochemical potentials slightly above 4.0 V vs Li^+/Li [29]. In LiFSI-based electrolytes with high salt concentrations, the corrosion is, however, inhibited [28,30].

The problem of Al corrosion can also be overcome by using a mixture of salts. For example, $LiPF_6$ (lithium hexafluorophosphate) is proved to supress the named issue, as a passivation layer of AlF_3 is formed on the aluminium surface at high potentials [31]. Also, it was shown that the corrosion of the cathodic current collector is strongly influenced by oxidation of the solvent molecules under these conditions. If the latter does not occur, passivation of the Al current collector in the presence of PF_6^- anions is more efficient [32]. Logically, one could consider the advantages of mixing the $LiPF_6$ and LiFSI salts to formulate a sulfone-based electrolyte which would be both compatible with the graphitic anode and stable at cell voltages above 5.0 V. Interestingly, this kind of synergy has already been reported for carbonate-based electrolytes, but the focus was put on the graphitic cathode [17,33]. In our work, we assessed this concept for sulfone-based systems.

To summarise, current work is dedicated to development, characterisation and tests of sulfone-based electrolytes for dual-graphite batteries, relying on the synergy of PF_6^- and FSI^- anions. We showed that the studied electrolyte series exhibited oxidation stability over 5 V vs. metallic lithium, compatibility with the graphitic anode and negligibly small corrosion impact on aluminium. Lastly, the economical expediency was evaluated. The final comparison criteria can be formulated more laconically as Performance (specific characteristics delivered by the system) – Sustainability (long-term cyclic stability at various current densities and resistance to the corrosion) – Price (PSP).

2. Results and discussion

If we consider the possibility of practical application of the electrolytes discussed in this study, a basic economical criterion should also be defined. In terms of specific energy density compared to that of modern LIBs produced by industry, dual-ion batteries are close to the LFP-based ones (450–550 vs. 540 Wh•kg^{-1}, estimation is based on the cathode), which are also the most widely used in industry [28,30,34,35]. For preliminary comparison on the laboratory scale, we may assume the average cathode material loading of 5 mg•cm^{-2}, corresponding electrolyte volume of 100 μl, and 1 M $LiPF_6$/EC:DMC (1:1, vol.) electrolyte (LP30, EC – ethylene carbonate, DMC – dimethyl carbonate). From a rough calculation, the price of 3000 € per litre of electrolyte and corresponding amount of the LFP cathode powder can be obtained, if we take a look in the catalogue of Sigma Aldrich, one of the most renown chemical suppliers [36]. This will serve as a reference value for the analysis of costs given in Section 2.6.

2.1. On the importance of preparation protocols

The work on the specified electrolytes began in parallel with our earlier study dedicated to structural behaviour of the graphitic DIB cathode at elevated temperatures [37]. There, we revisited the 2 M $LiPF_6$/EMS electrolyte proposed by Seel and Dahn [11] for the supplementary kinetic studies. Note that we switched to molality ($mol_{salt}•kg^{-1}_{solvent}$) from molarity, since formally, molar concentration ($mol_{salt}•l^{-1}_{solvent}$) is temperature-dependent. Although it was possible to obtain similar values of specific capacity to those reported, the stability upon cycling was never achieved (Fig. 1a). In the original publication, cell assembly was described as being done under an elevated pressure of ca. 10 bar for 20 min, which guaranteed proper wetting of the separator and electrodes. In our case, visually, the electrolyte was well-absorbed by the separator after about thirty seconds, and pressure applied to the cells during assembly was expected to assist with wetting of the electrodes. However, after the first few charge-discharge cycles, the characteristics dropped drastically, while the original work reported stable electrochemical cycling. The reason was unclear, until an electrochemical cell with the same electrolyte was tested after a few days of storage. In this case, the cycling stability became reproducible (Fig. 1b). Similar effect was observed when the formation cycles were conducted straight after assembly of the cells, and before further tests, these cells were left overnight. Recently, a study has been published, where the impact of the formation cycle conditions on the exfoliation of a graphitic anode was systematically investigated [38]. There, it has been clearly shown that preparation procedures play one of the key roles in the improvement of long-term performance of a battery system. Same effects, thereby, should be expected for the graphitic cathode. In our case, it is most likely related to the better penetration of the electrolyte into the pores of active material with increased storage time, as 2 m $LiPF_6$/EMS is a rather viscous liquid, with $\eta = 201.3$ mPa•s at 293 K (Fig. S1 and Table ST1). For the systems with modified electrolyte compositions, the preparation protocol was also found to be imperative, as shown in Section 2.4.

2.2. Basic physicochemical characterisation of the electrolyte series and approaches for their improvement

Although long-term cyclic stability might be achieved for the *Li|2 m $LiPF_6$/EMS|graphite* cells at low current densities, their characteristics drop drastically when the current is increased. The reason for this is a relatively low specific electrical conductivity σ of the named electrolyte. At 293 K, it equals 0.64 $mS•cm^{-1}$, which is more than an order of magnitude lower than that of the commonly used LP30 electrolyte (ca. 14 $mS•cm^{-1}$ [39]).

Replacement of $LiPF_6$ by LiFSI led to a significant decrease of dynamic viscosity (201.3 down to 66.0 mPa•s, Table ST1) and specific electrical conductivity of the electrolyte. The latter at 293 K is equal to 1.52 $mS•cm^{-1}$ for the 2 m LiFSI/EMS mixture, meaning more than double increase in comparison to the initial composition. This is related to the weaker interaction between Li^+ and large FSI^- species in the solution compared to that between Li^+ and smaller PF_6^- species. However, FSI^- anions are known for their corrosive activity against aluminium current collector [29], which was confirmed by low-rate cyclic voltammetry.

We compared specific electrical conductivities and corrosive activities for various ratios of LiFSI and $LiPF_6$ salts in the 2 m EMS-based solutions. The goal was to find the optimal ratio, which would offer a combination of a decent σ value combined with stability of the system at electrochemical potentials exceeding 5.0 V vs. Li^+/Li. The next step was to check the same parameters for the found ratio of the salts, but for the electrolyte based on another, preferably, a cheaper solvent of the same chemical nature. Later, the prepared electrolytes were tested in dual-ion cells with a graphitic cathode and lithium anode. The results of basic physicochemical and electrochemical characterisation are summarised in Table 1, Fig. 2 and supplementary Fig. S1 and Table ST1. As expected,

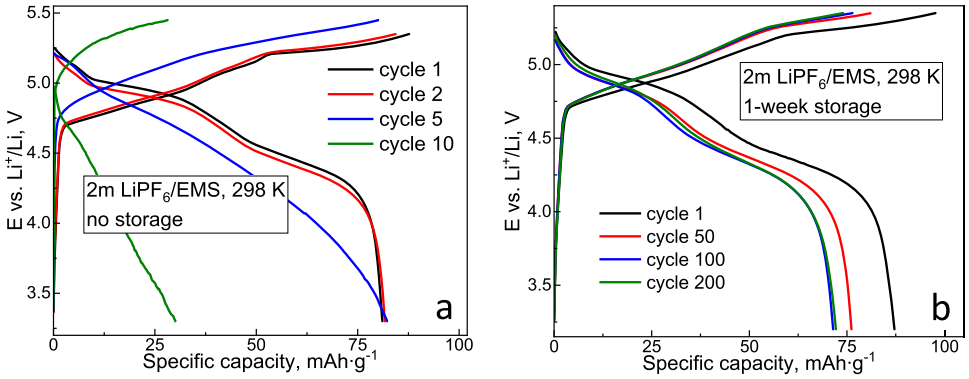

Fig. 1. The impact of storage of the electrochemical cells with EMS-based electrolyte before testing on subsequent cycling performance. Formation cycles are shown in SI.

Table 1
Specific electrical conductivities of the 2 m sulfone-based electrolytes with a mixture of $LiPF_6$ and LiFSI salts. Naming: "solvent/anion (FSI:PF_6 ratio)". Data points which were not included into the Arrhenius plots are shown in red.

Electrolyte → T, K ↓ σ, $mS•cm^{-1}$ ↘	EMSPF6	EMS13	EMS11	EMS31	EMSFSI	SL31
253	0.030(14)	0.0589(4)	0.080(4)	0.0409(3)	0.168(12)	0.22(10)
263	0.044(4)	0.137(10)	0.17(2)	0.1358(5)	0.330(3)	0.38(11)
273	0.137(2)	0.285(2)	0.33(3)	0.424(6)	0.585(9)	0.601(6)
283	0.362(7)	0.534(9)	0.610(12)	0.768(3)	0.97(15)	0.92(2)
293	0.64(14)	0.925(7)	1.010(5)	1.22(2)	1.52(2)	1.37(2)
303	1.07(12)	1.46(3)	1.570(12)	1.816(3)	2.27(4)	1.94(2)
313	1,67(2)	2.16(12)	2.310(10)	2.56(2)	3.150(9)	2.7(11)
323	2,47(2)	3.05(15)	3.20(2)	3.42(4)	4.23(8)	3.6(14)
333	3.41(3)	4.13(2)	4.30(6)	4.5(10)	5.55(9)	4.7(2)
E_a(diff), eV →	0.362(9)	0.38(13)	0.36(10)	0.30(11)	0.319(9)	0.278(3)

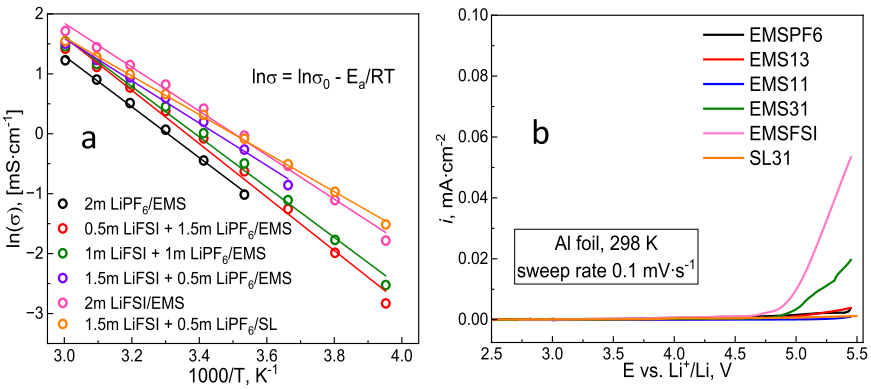

Fig. 2. (a) – Arrhenius plots of specific electrical conductivities for six studied sulfone-based electrolytes; (b) – linear sweep voltammograms in the high-voltage range.

the specific electrical conductivity of the 2 m EMS-based electrolytes at near-room temperatures grows along with the increase of LiFSI amount. Apart from that, the values of σ served as an indirect way of assessing the lower limit of operational temperature for members of the studied series. Drastic drop of the conductivity at a certain (reduced) temperature shown in Fig. 2a, means that the system is either frozen partially, becoming biphasic, or completely. Thus, we could confirm, that the 2 m $LiPF_6$/EMS (EMSPF6) electrolyte was not applicable at temperatures below 273 K. All mixtures containing the LiFSI salt follow the trend of conductivity increasing along with the FSI^-/PF_6^- ratio in the temperature range of 273 – 333 K. However, the tendency breaks at lower temperatures, with local maxima of conductivities for the 1 m LiFSI + 1 m $LiPF_6$/EMS electrolyte (EMS11). This points on the complexity of the ternary $LiPF_6$ – LiFSI – EMS system in terms of competitive ion-dipole, ion-ion and dipole-dipole interactions. One may assume that EMSPF6 and EMS31 stop being single-phase liquids at 263 K, which causes a dramatic decrease of their σ values.

Activation barriers for the ionic diffusion estimated from the Arrhenius plots, change non-monotonously. For example, 25% replacement of $LiPF_6$ by LiFSI in the EMS-based mixture led to a slight increase of E_a (0.38 eV for the EMS13 vs. 0.36 eV for the EMSPF6). The lowest barrier of 0.30 eV was calculated for the EMS31 mixture. We could expect this electrolyte to deliver the best performance among the series of mixtures in dual-ion batteries with a graphitic cathode. The consequence of replacing ethyl methyl sulfone by sulfolane, a common solvent in chemical industry [40], and thereby, beneficial in terms of price [36] for the 1.5 m LiFSI + 0.5 m $LiPF_6$ ratio was an increase in specific electrical conductivity for all temperatures, at which the measurements were done. Apart from that, a significant decrease of the E_a took place. The calculated value was 0.278 eV for the SL31 electrolyte (1.5 m LIFSI + 0.5 m $LiPF_6$ in sulfolane).

Further, we assessed the sulfone-based electrolytes series in terms of oxidation stability as well as stability of the aluminium cathodic current collector against corrosion at high electrochemical potentials. These may be reliably evaluated by low-rate linear sweep voltammetry. Panel b of Fig. 2 represents the results of these measurements. As one can see, a significant current increase is observed at around 4.9 V vs. Li^+/Li upon addition of a significant amount of LiFSI (EMS31 electrolyte). This is a definite confirmation of the Al current collector corrosion in the presence of FSI^-, as described in work [29]. When only FSI^- anions are present in the solution, the corrosive process becomes noticeable at around 4.65 V vs. metallic lithium.

Interestingly, for the same 3:1 ratio of LiFSI and $LiPF_6$, the initial corrosive current appears to be much lower in sulfolane then in ethyl methyl sulfone. At 5.45 V, the corrosive current density is slightly over 1 $\mu A \bullet cm^2$, which is around 0.6% of the lowest current densities in the galvanostatic charge-discharge experiments shown in *Sections 2.3* and *2.4*. To be more precise, the minimal current density was equal to 164 $\mu A \bullet cm^{-2}$ for the electrodes of 12 mm diameter and ~5 mg loading of the electrode composite. The estimated corrosion impacts the coulombic efficiencies of galvanostatic charge-discharge process for the cells shown in those sections. However, one should note that generally, the corrosion impact should be much lower in case of Al foil covered with the electrode composite compared to the bare foil served for the model studies. Besides, parasitic current in the SL31 electrolyte becomes noticeable only above 5.3 V, and such cells are subjected to this potential for a rather short time period. Finally, passivation of the current collectors in the presence of PF_6^- anions should take place upon cycling. Thus, loss of coulombic efficiency at lower currents should rather be caused by other undesired reactions in the cells, or, more likely, by kinetic complications of the solid-state diffusion than by the Al corrosion only.

The 1.5 m LiFSI + 0.5 m $LiPF_6$/SL electrolyte seemed to be the most preferred both in terms of electrical conductivity and resilience of the Al current collector to corrosion. The possibility of making the sulfone-based electrolyte series compatible with metallic lithium was indirectly proved by the long-term cycling of the *Li-graphite* half-cells after optimisation of the preparation protocol, as shown in *Sections 2.1* and *2.3*. However, even for the SL31 electrolyte, selected as the most promising one after the preliminary studies, the disadvantage of relatively low specific electrical conductivity remained. Here, a fundamental physicochemical approach might be considered to expand the temperature window of operation for the sulfone-based electrolytes. The components of these electrolytes: $LiPF_6$, LiFSI, SL, EMS, are able to form eutectic mixtures [41,42]. For the optimal ration of the electrolyte salts, we investigated some effects of using the eutectic mixture of EMS and SL as a solvent.

As seen from our differential calorimetry (DSC) experiments, EMS – SL represent a system with a simple eutectic (Fig. 3). EMS has a melting point of 310 K, which makes it applicable as a solvent only when the electrolyte salt is added. For sulfolane, this value is less defined. At 298 K it is an oily amorphous substance. While many suppliers state its melting point to be slightly above the room temperature, the results of differential scanning calorimetry (DSC), which was conducted to build the phase diagram of the EMS – SL binary system, revealed the value of about 290 K. In fact, this result agrees with literature, where the difference between the melting (301 K) and transitional (288 K) temperatures are explained by the globular properties of SL molecules [43,44]. These globular properties of SL molecules can explain the anomalously high electrical conductivity of the SL31 electrolyte compared to that of EMS31. While EMS and SL have comparable dielectric constants ($\varepsilon = 57.5$ and 42.9, respectively [20]) and dipole moments (both $\mu > 4.5$ D), the molecular structure of sulfolane tends to hinder influence of the positive pole [40], thus one can expect a weaker interaction between SL molecules and anions compared to that in case of EMS. Also, it is important to note that these parameters of sulfolane should depend on its purity, and chemical nature of the admixtures, in other words, on the supplier.

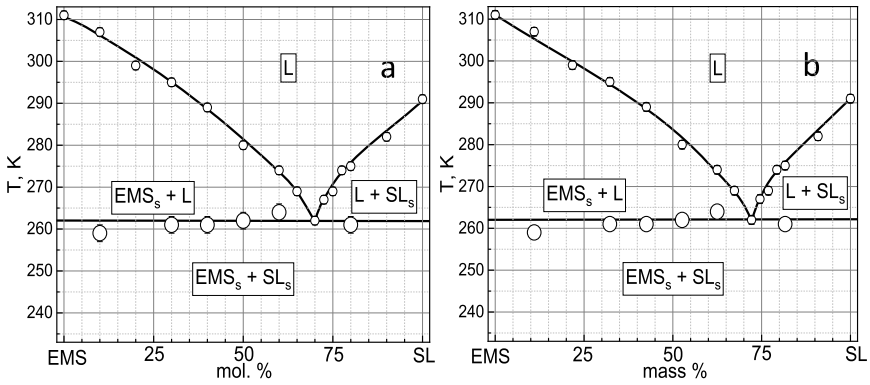

Fig. 3. Phase diagram of the binary ethyl methyl sulfone – sulfolane system. (a) – molar fractions, (b) – mass fractions. Points on liquidus and solidus lines are displayed concerning the highest error in the series: ±1 K for the liquidus and ±2 K for the solidus.

In our DSC results, on the curve corresponding to temperature elevation, two endothermic peaks were observed for sulfolane: the big one, with a maximum at about 290 K, and a much smaller one, with a maximum at 296 K. The first one can be attributed to the melting point of sulfolane. The smaller peak corresponds to melting of the admixtures (Figure S2a). In the presented phase diagram, we considered the first peak as the melting point of sulfolane, accounting for its upper-mentioned nature at the given temperature. Another characteristic feature of this system is the tendency to form supercooled liquids. Hysteresis between melting and freezing processes was observed for both end-members of the row, as well as for all their mixtures. This agrees well with an earlier report dedicated to the ethylene carbonate – sulfolane binary system [45]. Thus, we considered the heating part of DSC curves for defining the points of the liquidus curve. Two endothermic peaks are visible on each one, except for pure EMS and the eutectic mixture (Figure S2b, c). Following the general practice [46], we took onsets of the first endothermic peaks as solidus temperatures, and maxima of the second endothermic peaks as liquidus. Corresponding values are available in the supplementary file (Table ST2). A mixture consisting of 70 mol. % (72 mass %) sulfolane and 30 mol. % ethyl methyl sulfone was found to be the eutectic with a melting point of 262 K, which fulfils the goal of broadening the temperature window of operation for the sulfone-based electrolytes. Besides, electrolytes with this mixture serving as a solvent, could still be economically beneficial, since the mass fraction of EMS is low.

Certainly, lowering the melting point of the solvent for a given salt (or ratio of salts) does not necessarily guarantee the improvement of electrolyte characteristics. In the case of a single salt – binary solvent system or binary eutectics, this approach can be applied relatively directly, allowing to broaden the operating temperature window for the electrolyte [41,42,45]. In our case, we deal with two salts, so the system becomes quaternary, and given the significantly different solubility of $LiPF_6$ in EMS and SL [41,42], one cannot conclude a noticeable drop of viscosity and increase of the electrical conductivity just from lowering the solvent's melting point. Nevertheless, for the electrolyte with high amount of $LiPF_6$, EMS13, certain improvement was achieved. Firstly, from the economical point of view, the replacement of 72 mass % EMS by SL is beneficial. Secondly, the possibility of dissolving a sufficient amount of $LiPF_6$ remained, which is advantageous in terms of preventing the Al corrosion. However, the impact of solvent replacement on the electrical conductivity was not direct. Slight increase of the σ values was observed at temperatures below 273 K for the 0.5 m LiFSI: 1.5 m $LiPF_6$ ratio (see Table ST3). For the ratio of 1.5 m LiFSI: 0.5 m $LiPF_6$, the replacement of EMS by the eutectic mixture led to more than a double increase (0.094 vs. 0.041 mSm•cm^{-1}) at 253 K. Both mixtures exhibited a slight loss in conductivity above 273 K compared to the electrolytes with a singular EMS solvent. It appears that for the selected mixture of salts, simple use of a singular solvent with a lower melting point is more beneficial, as the SL31 electrolyte outperformed all the other candidates. For the future studies, search for ternary eutectic of the LiFSI – $LiPF_6$ – SL system can be proposed. Although requiring a significant effort in search, this eutectic mixture might be the best among the electrolyte compositions within the system in fulfilling the earlier formulated "PSP" criteria. One can also try reducing the overall salt concentration to decrease the electrolyte viscosity and increase its conductivity (Figure S3a, Table ST3), but this results in a significant loss of coulombic efficiency at relatively low currents compared to the initial 2 m LiPF6/EMS electrolyte (Figure S3b) due to increased impact of parasitic reactions in the cell. Long-term stability at higher current densities decreases as well (Figures S3c-d).

The next step of this work was to subject the most promising electrolyte-candidate to tests in dual-ion cells for its long-term performance evaluation. The same was done for the remaining members of the series.

2.3. *Long-term cycling at a moderate current density*

Although electrochemical cycling of graphitic cathodes for DIB at high currents is beneficial for several potential applications, as well as in terms of reducing the impact of corrosion, and subsequently, improvement of the coulombic efficiency, the stability of these systems at low current densities is imperative, since normally, even if charged fast, the batteries are supposed to be discharged within a relatively long time. If we consider the industry of electric vehicles, most of the modern standard battery testing protocols are limited by current densities between 0.3 and 2C [47]. Here, 1C corresponds to the current required for a complete charge or discharge of the electrochemical cell within an hour.

An additional comment has to be made on calculations of the theoretical specific capacity values for graphite in case of anionic intercalation. Unlike for state-of-the-art cathodes, the exact compositions of graphite anionic intercalation compounds are not defined that well. Typical example is C_xPF_6, for which the x value was assumed to be 16, 18, and 20 as the final electrochemically achievable stage. These assumptions were made after applying a variety of theoretical and experimental methods, the latter in different conditions [11, 48–51]. Therefore, referring to the current densities instead of C-rates would be more correct.

Typical galvanostatic charge-discharge curves for graphite-Li cells with the sulfone-based electrolytes are presented in Fig. 4, and the extended information is available in the SI file (Figures S4, S5). The average anionic intercalation potential decreased along with increasing the amount of LiFSI in the system. Complete replacement of $LiPF_6$, resulted into a significant drop of coulombic efficiency, which is explained by a more pronounced corrosion of the Al current collector in the presence of FSI^- anions. However, the contribution of corrosion for the cells with EMSFSI electrolyte can be significantly reduced at

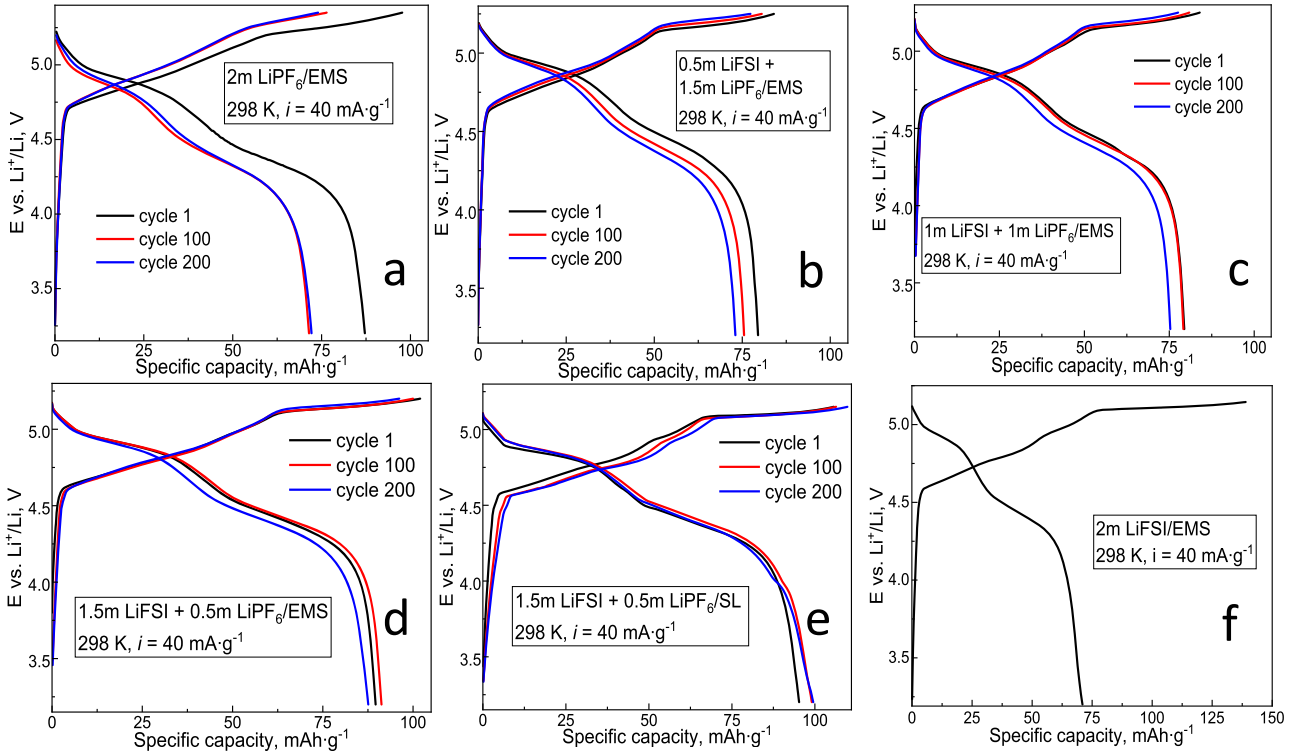

Fig. 4. Typical galvanostatic charge-discharge curves corresponding to long-term cycling of the graphitic cathode in series of 2 m sulfone-based electrolytes at current density of 40 mA•g^{-1}. For the 2 m LiFSI/EMS electrolyte (f), a singular cycle is shown to illustrate the impact of corrosion.

relatively high currents. Thus, at 280 mA•g^{-1}, the coulombic efficiency of up to 98% can be reached for this mixture (Figures S4b, S5f). Nevertheless, a significant concentration of PF_6^- has to be present to achieve stable cycling at low current densities. For the cells with mixed-salt electrolytes based on ethyl methyl sulfone cycled at 40 mAh•g^{-1}, the coulombic efficiency (CE) varied from 92 to 98% (Figure S5a-e), which exceeds or is the same with the values reported in recent studies, where higher current densities were applied and carbonate-based electrolytes were used [17,30,33]. Although higher CE values were shown by the cells with higher concentrations of PF_6^- anions, the most stable cycling was exhibited by those with the 1.5 m LiFSI + 0.5 m $LiPF_6$/EMS electrolyte. Also, such cells delivered the highest values of specific discharge capacity during the preliminary tests. This is explained by combination of factors. The impact of parasitic electrochemical reactions in the cell caused by FSI^- anions remained relatively low, while physicochemical properties of the electrolyte improved: reduced viscosity, increased ionic conductivity and surface wetting of graphite (was evaluated visually, see Figure S6) influenced the overall performance positively. After 300 cycles at 40 mA•g^{-1}, the discharge capacity decreased from 90 to 86 mAh•g^{-1}, meaning about 95.6% retention (Figure S5e). Cells with concentration of $LiPF_6 \geq 1$ m tend to lose cyclic stability more rapidly (Figure S5a-c).

Electrochemical cells with the 1.5 m LiFSI + 0.5 m $LiPF_6$ mixture in sulfolane, which was initially selected as the most promising electrolyte-candidate, outperformed the EMS-based series in terms of delivered specific characteristics, as well as long-term behaviour. After being subjected to the same number of charge-discharge cycles, the cells delivered 98.0% capacity retention. The coulombic efficiency varied between 92 and 94% (Figure S5e). One of the reasons for this should be laying in the lowest activation barrier for ionic diffusion in the SL31 electrolyte among the whole series. From the preliminary evaluation, this electrolyte looked the most promising for DIBs, concerning both the performance and economical aspect.

2.4. Optimisation of the preparation and cycling protocols

Carefully selected voltage window is one of the key factors defining the long-term performance of a battery system. In case of electrochemical anionic intercalation, the upper voltage cut-off seems to be even more crucial. Generally, this parameter should be set based on the balance between the achievable energy density and undesired side reactions, represented by corrosion of the current collector and (or) decomposition of the electrolyte. Numerous works report excellent stability of the current collector and electrolyte within the given voltage range for the super-concentrated electrolytes [13,14]. Therefore, the origin of the reduce in reversibility of the electrochemical insertion of anions to stages with low number *n* remains uncertain. Apart from the side reactions, partial trapping of the intercalated anions in between graphene layers [51] as well as co-intercalation of solvent molecules

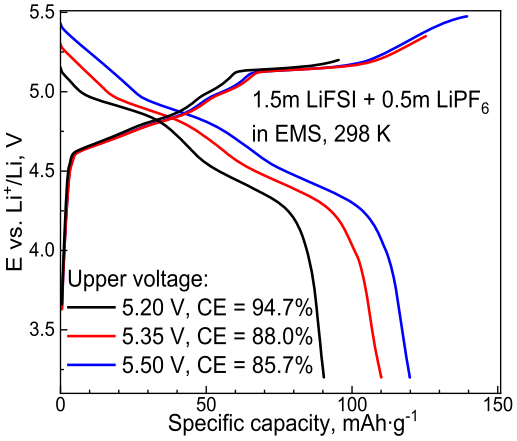

Fig. 5. The effect of increasing the upper voltage limit for EMS31. Current density: 56 mA•g^{-1}.

might take place [50,52]. All of that, together with uncertainty of the exact chemical compositions of anionic GICs, complicates the development of cycling protocols. Thus, a proper choice of the voltage cut-off for operation of the graphitic cathode at various currents could be done only by trial and error. Fig. 5 represents a typical example of such selection. As shown in the previous section, the cells with the 1.5 m LiFSI + 0.5 m $LiPF_6$/EMS electrolyte were charged up to 5.15 V vs. lithium with a current density of 40 mA•g^{-1}, allowing a discharge capacity of 90 mAh•g^{-1}, good cyclability and a coulombic efficiency exceeding 92%. If these cells are subjected to higher currents, polarisation increases, and the intercalation process requires higher voltages. When the upper voltage was increased to 5.35 and 5.5 V from the initially chosen 5.20 V (Figure S4c) for cycling at a slightly increased (56 mA•g^{-1}) current density, the reversible specific capacity values grew to about 110 and 120 mAh•g^{-1}, respectively, and remained relatively stable. However, the coulombic efficiency dropped below 90%. The most obvious explanation for that would be increased contributions of currents from corrosion of the Al current collector and (or) solvent decomposition. Although these should definitely take place, it is important to compare the shapes of charge-discharge curves. From Fig. 5 it is clear, that the shape of the charging curve did not change much with the upper voltage increase and it was reproducible for multiple cycles (Fig. S2c), whereas the polarisation of the cell decreased: discharge occurred at higher voltages in the second case. Thus, it would be logical to assume that the part of the charge curve between 5.35 and 5.5 V is dominated by the anionic intercalation. Note, the latest theoretical calculations propose the final composition of C_{12}FSI for FSI-based GIC [48,49], which would correspond to a specific charge capacity of 187 mAh•g^{-1}. The values we were able to obtain in this experiment, correspond to compositions of C_{16}(FSI, PF_6) on charge and roughly to C_{18}(FSI, PF_6) on discharge. Thus, we might suppose that the charge process was ended at the beginning of the intercalation stage 1 (or more generally, the maximal intercalant concentration stage MIC [37]) formation. This assumption, however, requires confirmation by more sophisticated experimental methods.

Certainly, if the current density is increased, the relative contribution of parasitic electrochemical reactions should decrease accordingly, allowing to charge the studied dual-ion cells to higher voltages, thus achieving higher reversible specific capacities and coulombic efficiencies. On the other hand, this should result in an increased polarisation and a more rapid decay of the specific characteristics due to inhomogeneous distribution of the intercalant species in graphite, subsequently causing exfoliation. Additionally, the increased polarisation might lead to inaccessibility of the stages with a low number *n* upon cell charge. One should expect the polarisation issue to be more critical for the electrolytes with relatively low conductivities, to which the studied series belong. At this point, we also investigated the impact of storage time onto polarisation of the graphitic cathode during charge. Fig. 6 is demonstrating the influence of the upper voltage cut-off as well as the storage time before electrochemical tests on performance of the cells with the 1.5 m LiFSI + 0.5 m $LiPF_6$/SL electrolyte. Supplementary file contains the same information for the EMS-based series (Figure S7).

As visible from panel a, without improvement of charge-discharge and preparation protocols, decent specific characteristics and cyclability can be achieved at moderate current densities. When the latter is increased, polarisation of the cells grows significantly, making the intercalation to stage 2, represented by the last plateau on the charge curve, impossible, and the process ends at stage 3. Although the cycling stability remains, at current densities above 100 mA•g^{-1}, such cells deliver between 0.5 and 0.6 of their discharge capacity obtained at lower currents. Nevertheless, when the current is reduced again, the initial values are retained. Increase of the upper voltage cut-off (panel b) results into broadening of the currents range, under which a decent electrochemical performance is exhibited. However, the issue of polarisation is still present.

Storage of the assembled cells for longer time (panel c) resulted in a significant improvement of all parameters. The most noticeable effect was reduced polarisation of the cells with current increase. It allowed to achieve even higher specific characteristics at 280 mA•g^{-1} current than those at 40 mA•g^{-1}, probably due to the reduced impact of corrosion. Apart from that, an exceptional capacity retention was achieved for hundreds of cycles (panel d). In this case, one could potentially assume the pseudocapacitive phenomenon [53] participating in the charge

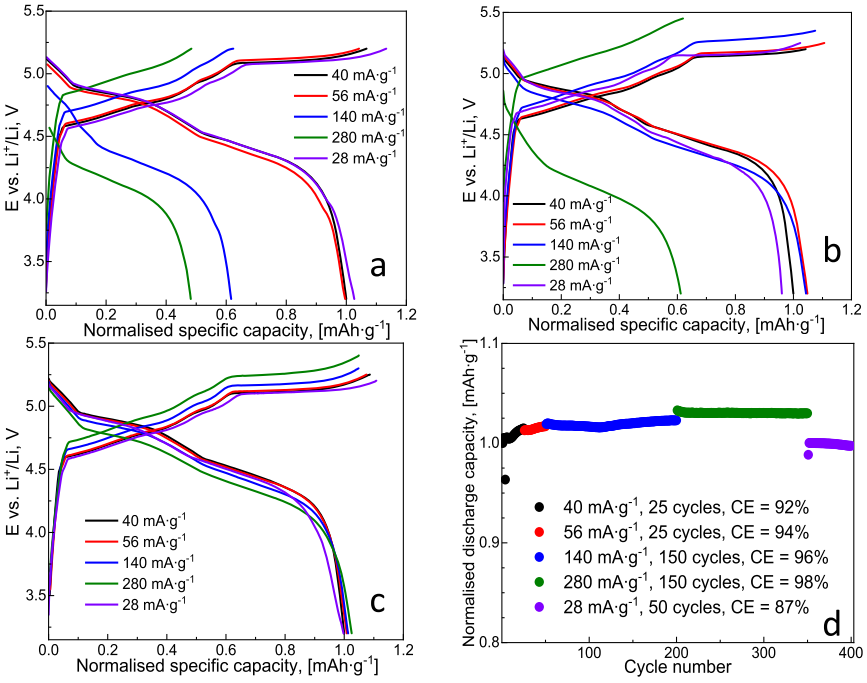

Fig. 6. The effects of preparation and testing protocol on the electrochemical behaviour of graphite as a cathode in Li-cells with the 1.5 m LiFSI + 0.5 m $LiPF_6$/SL electrolyte. (a) – storage overnight after formation cycle, no upper voltage cut-off optimisation; (b) – storage overnight after formation cycle, optimised voltage cut-off; (c) – 1-week storage, optimised voltage cut-off; (d) – long-term performance of a typical cell shown in panel (c). The capacity was normalised on the number obtained statistically after cycling of 10 cells at 40 mA•g^{-1} current density, equal to 94±5 mAh•g^{-1} (see the SI for the procedure).

storage or even a classical capacitive energy storage mechanism. However, the specific surfaces of all cathode composite components are rather low (74 $m^2 \bullet g^{-1}$ for KS6L and 54 $m^2 \bullet g^{-1}$ for C65, Table ST4 and Figure S8) compared to that of activated carbons (> 500 $m^2 \bullet g^{-1}$ [54]), and the named effects are expected to be negligibly small.

For basic evaluation of storage effects on the Li-anode, we conducted a series of EIS experiments under blocking conditions (0% state of charge) of the freshly assembled cells with EMSPF6, EMS31 and SL31, the same cells straight after formation cycle and finally, after subsequent storage. The results are available in the supplementary file (Fig. S9). Although complicated assumptions would be inconclusive, some preliminary ones can be made. In the case of 2 m $LiPF_6$/EMS electrolyte, charge transfer resistance attributed to the Li-electrolyte interface was stable straight after assembly of the cells. It increased significantly after the formation cycle, but tended to decrease during storage. As the most general outcome, we may assume that formulation of SEI on the Li-anode continues after the formation cycle is over, and storage is required for this process to complete. After additional 12 h, the tendency of decreasing charge transfer resistance remained, but was much less pronounced.

In the case of EMS31 and SL31, the situation got more complicated. Despite the better electrochemical performance of such cells compared to the EMSPF6-based ones, the charge transfer resistance on the Li-electrolyte interface appeared to grow over time under the same conditions. However, as stated earlier, the impact of long-term storage was found to be positive for them as well. Strong decrease of the low-frequency component was observed for these electrolytes too. Probably, this is caused by some anions trapped in the host structure of graphite. Nevertheless, the positive impact of storage on the resulting performance was observed without conducting the formation cycle beforehand. Decrease of the low frequency component seems to be critical at the end, but the reasons for its decrease remain uncertain. Comprehensive understanding of the processes occurring on the electrode-electrolyte interface would therefore require a separate electrochemical study.

2.5. Compatibility with a graphitic anode and metallic lithium

As specified in the introduction, one of the main disadvantages of sulfones as electrolyte solvents is their instability against reduction at low potentials. Presence of FSI^- anions in the electrolyte series investigated within the frame of this study allows to overcome this issue, as shown in Sections 2.2 and 2.3 by long-term cycling of half cells with graphite serving as a cathode. Since part of the concept, being targeted by development of these series, represents reduction of lithium consumption, it was essential to assess the compatibility of EMS- and SL-based electrolytes also with a graphitic anode. Fig. 7 is demonstrating the results of such tests for the 1.5 m LiFSI + 0.5 m $LiPF_6$/SL electrolyte. The same was done with the EMS31 mixture, however the results were less satisfactory (Fig. S10).

Panel a is illustrating the effect of storage of the assembled half-cells on the formation cycle for the graphitic anode in the named electrolyte. It appears that the storage effect is much less pronounced in this case compared to that with graphitic cathode: the coulombic efficiency of the first formation cycle improved only slightly, from 78 to 82%; the number of cycles (about 10), required to achieve the stable capacity and coulombic efficiency close to 100%, as shown in panel b, remained unchanged after 1-week storage. The values of initial coulombic efficiency on the formation cycles are comparable to that in most of conventional LIB electrolytes [55], and excellent capacity retention is obtained at current densities corresponding to those in the cells tested in Section 2.3. Clearly, the SL31 electrolyte is compatible with a graphitic anode, and after a further optimisation, it could be used in dual-graphite cells.

2.6. Estimations of costs

After selecting the best-performing sulfone-based electrolytes, we can assess them in terms of price. For LFP-based Li-ion batteries, the cost strongly depends on that of the cathode material, while for sulfone-based dual-ion batteries, the price is defined by the electrolyte. The comparison based on the earlier set laboratory-scale parameters, is presented in Table 2. In the calculations, we neglected the low price of graphitic cathode.

One can see that among Li-based electrolytes for dual-ion cells with graphite as a cathode, proposed by several reference works [15,17,34], only those with super-concentrated 4 M $LiPF_6$ in DMC [15] are cheaper

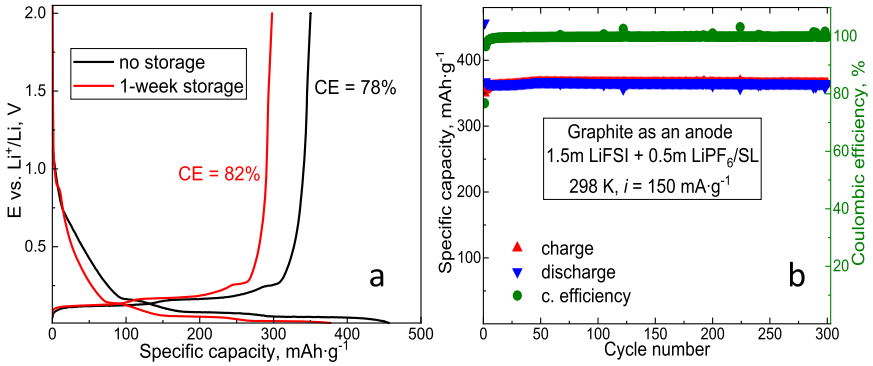

Fig. 7. (a) – the impact of storage time on the coulombic efficiency of the first formation cycles for graphitic anodes in the 1.5 m LiFSI + 0.5 m $LiPF_6$/SL electrolyte at a current density of 150 $mA \bullet g^{-1}$; (b) – long-term cycling behaviour.

Table 2
Preliminary comparison of prices for LFP-based batteries and graphite dual-ion cells.

Cathode	Electrolyte	Electrolyte price (Sigma Aldrich), €/litre	1 L of electrolyte + 70 g of cathode price (lab scale), €
$LiFePO_4$	1 M $LiPF_6$/EC:DMC (1:1 vol.) (LP30)	1300	3000
graphite	4 M $LiPF_6$/DMC [15]	2400	2400
	5 M LiFSI + 2 M $LiPF_6$/EC:DMC (1:1 vol.) [17]	10,500	10,500
	1 M LiTFSI in $Pyr_{14}TFSI$*, [34]	7800	7800
	2 m ($LiPF_6$ + LiFSI)/EMS, this study	6000	6000
	2 m ($LiPF_6$ + LiFSI)/SL, this study	2400	2400

* Estimations are based on the other supplier (TCI Chemicals), with higher quantity and purity of reagents available. The price of graphite is neglected.

than the LFP-based ones (20% advantage in costs). However, as specified earlier, specific characteristics of graphite in this electrolyte are more moderate than in sulfone-based ones. Electrolytes with higher concentration of lithium salt (7 M, [17]) exceed the price of the LFP-based system several times. An ionic-liquid-based alternative, despite its promising performance [34], suffers from the same drawback.

If we consider the 2m-concentrated EMS-based electrolyte series on the laboratory scale, we double the costs compared to the LFP-based reference. However, for the same salt concentration, the replacement of EMS by SL is price-beneficial: a system based on a graphitic cathode and the SL31 electrolyte is 20% cheaper than the one based on LFP and LP30. Noteworthy, higher loadings of the electrodes, more relevant for potential industrial applications, would be profitable for the graphite-sulfone electrolyte combination. Thus, if the electrode loading is doubled (keeping the electrolyte volume unchanged), the cathode-electrolyte price for the LFP-reference increases to 4700€, making the sulfolane-based electrolyte even more competitive from the economical point of view, especially, if the recycling costs are accounted for. Lastly, we must make a note of caution, since the prices of the reagents for laboratory and industry might differ strongly, and also can change quickly. Therefore, we highlight that the given price estimations are approximate, and serve primarily to demonstrate the importance of the economical factor for electrolytes' development.

3. Conclusion

In our study, we demonstrated the principal possibility of making practice-relevant sulfone-based electrolytes for long-term cycling of dual-ion batteries with a graphitic cathode. These electrolytes were made compatible with both metallic lithium and graphite, serving as anodes, by applying the synergy of two lithium salts: $LiPF_6$ and LiFSI. The first one was necessary to passivate the cathodic current collector during the formation cycles, whereas the second one assured the stability of sulfones against reduction at low potentials. We were able to avoid using the concept of super-concentrated electrolytes, which resulted in improvement of specific characteristics of the graphitic cathode. Several hundreds of electrochemical cycles at various current densities with high coulombic efficiencies are possible for such battery cells. Current densities in between 100 and 300 $mA \bullet g^{-1}$ were found to be optimal. If lithium metal is used as an anode, such cells can already be upscaled for practical applications, the ones with a graphitic anode would require additional optimisation, especially in terms of preparation protocol. This might include putting the assembled cells under slightly elevated temperatures to reduce the storage time before electrochemical procedures, or pre-cycling of the graphitic anode. We expect that the time required for proper wetting of the electrodes by sulfone-based electrolytes might be significantly reduced, if the assembled cells are stored at a moderately elevated temperature. This is particularly important for improving the previously mentioned practical expediency. Such investigations are considered for further research on the system.

Furthermore, it was possible to develop a sulfolane-based electrolyte, competitive from economical aspects, as well as in terms of performance. Since the family of sulfones contains a lot of compounds, an even cheaper one (or a mixture of sulfones) can be selected as the solvent. We assessed the perspectives of improving the studied electrolytes through a fundamental approach. In particular, we conducted a primary physicochemical investigation of the binary ethyl methyl sulfone – sulfolane system, and built its phase diagram with a binary eutectic point defined, purposing to broaden the operating temperature window of the dual-ion batteries from current work. This approach, however, is not straightforward in application, as it was shown by the subsequent conductivity measurements, and requires an extended study, such as investigating the ternary systems of a type binary salt – singular solvent.

Extensive studies involving EIS at various states of charge, post-mortem SEM, TEM, XPS, as well mass-spectrometry during cell operation, to target the possible formation of an artificial solid electrolyte interface on the anode of DIB and cathode electrolyte interface on its positive electrode during storage, will be the main subject of follow-up papers, as well as processes occurring on both electrodes upon long-term cycling in the sulfone-based electrolyte series. Special focus will be put onto influence of the storage conditions on the latter and the resulting battery behaviour. Finally, the electrolytes presented in this work might find applications in other high-voltage batteries, for example, with Li-NMC cathodes, although their low electric conductivity might be an issue. Another interesting direction would be to expand the proposed electrolyte concept onto dual-ion systems with other alkali-metals.

CRediT authorship contribution statement

Mikhail V. Gorbunov: Writing – review & editing, Writing – original draft, Validation, Methodology, Investigation, Formal analysis, Data curation, Conceptualization. **Cansin Bulut:** Investigation. **Daria Mikhailova:** Writing – review & editing, Validation, Project administration, Funding acquisition.

Declaration of competing interest

The authors declare that they have no known competing financial interests or personal relationships that could have appeared to influence the work reported in this paper.

Acknowledgements

This research benefitted from financial support of the DFG-448719339 project "KIBBS" and of the POLiS Cluster of Excellence (funded by the DFG, German Research Foundation, under Germany's Excellence Strategy - EXC 2154). The authors are grateful to Birgit Bartusch (IFW Dresden) for performing differential scanning calorimetry measurements and Tatiana Barantseva (KIT) for assistance with supplementary studies.

Supplementary materials

Supplementary material associated with this article can be found, in the online version, at doi:10.1016/j.electacta.2026.148788.

Data availability

Original data is available as an archive under following link:

References

[1] T. Kim, W. Song, D.-Y. Son, L.K. Ono, Y. Qi, Lithium-ion batteries: outlook on present, future, and hybridized technologies, J. Mater. Chem. A 7 (2019) 2942–2964, https://doi.org/10.1039/C8TA10513H.
[2] A. Yao, S.M. Benson, W.C. Chueh, Critically assessing sodium-ion technology roadmaps and scenarios for techno-economic competitiveness against lithium-ion batteries, Nat. Energy 10 (2025) 404–416, https://doi.org/10.1038/s41560-024-01701-9.
[3] T. Hosaka, K. Kubota, A. Shahul Hameed, S. Komaba, Research development on K-ion batteries, Chem. Rev. 120 (14) (2020) 6358–6466, https://doi.org/10.1021/acs.chemrev.9b00463.
[4] C. You, X. Wu, X. Yuan, Y. Chen, L. Liu, Y. Zhu, L. Fu, Y. Wu, Y.-G. Guo, T. van Ree, Advances in rechargeable Mg batteries, J. Mater. Chem. A 8 (2020) 25601–25625, https://doi.org/10.1039/D0TA09330K.
[5] I.D. Hosein, The promise of calcium batteries: open perspectives and fair comparisons, ACS Energy Lett. 6 (4) (2021) 1560–1565, https://doi.org/10.1021/acsenergylett.1c00593.
[6] T. Mageto, S.D. Bhoyate, K. Mensah-Darkwa, A. Kumar, R.K. Gupta, Development of high-performance zinc-ion batteries: issues, mitigation strategies, and perspectives, J. Energy Storage 70 (2023) 10801, https://doi.org/10.1016/j.est.2023.108081.
[7] G.A. Elia, K.V. Kravchyk, M.V. Kovalenko, J. Chacon, A. Holland, R.G.A. Wills, An overview and prospective on Al and Al-ion battery technologies, J. Power Sources 481 (2021) 228870, https://doi.org/10.1016/j.jpowsour.2020.228870.

[8] N. Nasajpour-Esfahani, H. Garmestani, M. Bagheritabar, D.J. Jasim, D. Toghraie, S. Dadkhah, H. Firoozeh, Comprehensive review of lithium-ion battery materials and development challenges, Renew. Sustain. Energy Rev. 203 (2024) 114783, https://doi.org/10.1016/j.rser.2024.114783.

[9] Z. Dobo, T. Dinh, T. Kulcsar, A review on recycling of spent lithium-ion batteries, Energy Rep. 9 (2023) 6362–6395, https://doi.org/10.1016/j.egyr.2023.05.264.

[10] F.P. McCullough, A. Levine, R.V. Snelgrove, *USPat.*, 4830938, 1989.

[11] J.A. Seel, J.R. Dahn, Electrochemical intercalation of PF_6 into graphite, J. Electrochem. Soc. 147 (2000) 892, https://doi.org/10.1149/1.1393288.

[12] H. Tian, M. Graczuk-Zajac, A. Kessler, A. Weidenkaff, R. Riedel, Recycling and reusing of graphite from retired lithium-ion batteries: a review, Adv. Mater. 36 (13) (2024) 2308494, https://doi.org/10.1002/adma.202308494.

[13] Y. Matsuo, A. Inoo, J. Inamoto, Electrochemical intercalation of anions into graphite: fundamental aspects, material synthesis, and application to the cathode of dual-ion batteries, Chem. Europe 13 (8) (2024) e202300244, https://doi.org/10.1002/open.202300244.

[14] S. Sayah, A. Ghosh, M. Baazizi, R. Amine, M. Dahbi, Y. Amine, F. Ghamouss, K. Amine, How do super concentrated electrolytes push the Li-ion batteries and supercapacitors beyond their thermodynamic and electrochemical limits? Nano Energy 98 (2022) 107336 https://doi.org/10.1016/j.nanoen.2022.107336.

[15] S. Künne, J.M. Hesper, T. Lein, K. Voight, D. Mikhailova, A. Michaelis, M. Winter, T. Placke, C. Heubner, Hybrid high-voltage $LiNi_{0.5}Mn_{1.5}O_4$/graphite cathodes enabling rechargeable batteries with simultaneous anion- and cation storage, Batter. Supercaps 6 (9) (2023) e202300284, https://doi.org/10.1002/batt.202300284.

[16] P. Münster, A. Heckmann, R. Nölle, M. Winter, K. Beltrop, T. Placke, Enabling high performance potassium-based dual-graphite battery cells by highly concentrated electrolytes, Batter. Supercaps 2 (2019) 992–1006, https://doi.org/10.1002/batt.201900106.

[17] D. Sabaghi, G. Wang, D. Mikhailova, A. Morag, A. Omar, D. Li, S. Khosravi Haji Vand, M. Yu, X. Feng, A. Shaygan Nia, High energy density and durable pouch-cell graphite-based dual ion battery using concentrated hybrid electrolytes, J. Power Sources 588 (2023) 233685, https://doi.org/10.1016/j.jpowsour.2023.233685.

[18] Y. Yamada, A. Yamada, Review – Superconcentrated electrolytes for lithium batteries, J. Electrochem. Soc. 162 (2015) A2406–A2423, https://doi.org/10.1149/2.0041514jes.

[19] N. Xin, Y. Sun, M. He, C.J. Radke, J.M. Prausnitz, Solubilities of six lithium salts in five non-aqueous solvents and in a few of their binary mixtures, Fluid Phase Equilib. 461 (2018) 1–7, https://doi.org/10.1016/j.fluid.2017.12.034.

[20] V.S. Kolosnitsyn, N.V. Slobodchikova, L.V. Sheina, Electroconduction of lithium perchlorate solutions in sulfones, Russ. J. Electrochem. 37 (6) (2001) 599–604, https://doi.org/10.1023/A:1016666517462.

[21] A. Abouimrane, I. Belharouak, K. Amine, Sulfone-based electrolytes for high-voltage Li-ion batteries, Electrochem. Commun. 11 (2009) 1073–1076, https://doi.org/10.1016/j.elecom.2009.03.020.

[22] N. Shao, X.-G. Sun, S. Dai, D. Jiang, Electrochemical windows of sulfone-based electrolytes for high-voltage Li-ion batteries, J. Phys. Chem. B 115 (42) (2011) 12120–12125, https://doi.org/10.1021/jp204401t.

[23] K. Xu, Nonaqueous liquid electrolytes for lithium-based rechargeable batteries, Chem. Rev. 104 (10) (2004) 4303–4418, https://doi.org/10.1021/cr030203g.

[24] M.M. Rahman, E. Hu, Electron delocalization enables sulfone-based single-solvent electrolyte for lithium metal batteries, Angew. Chem. Int. Ed. 62 (44) (2023) e202311051, https://doi.org/10.1002/anie.202311051.

[25] X. Ren, S. Chen, H. Lee, D. Mei, M.H. Engelhard, S.D. Burton, W. Zhao, J. Zheng, Q. Li, M.S. Ding, M. Schroeder, J. Alvarado, K. Xu, Y.S. Meng, J. Liu, J.-G. Thang, W. Xu, Localized high-concentration sulfone electrolytes for high-efficiency lithium-metal batteries, Chemistry 4 (8) (2018) 1877–1892, https://doi.org/10.1016/j.chempr.2018.05.002.

[26] P. Hilbig, L. Ibing, R. Wagner, M. Winter, I. Cekic-Laskovic, Ethyl methyl sulfone-based electrolytes for lithium ion battery applications, Energies 10 (9) (2017) 1312, https://doi.org/10.3390/en10091312.

[27] I.A. Shkrob, T.W. Martin, Y. Zhu, D.P. Abraham, Why Bis(fluorosulfonyl)imide is a "magic anion" for electrochemistry, J. Phys. Chem. C 118 (34) (2014) 19661–19671, https://doi.org/10.1021/jp506567p.

[28] X. Li, X. Ou, Y. Tang, 6.0 V high-voltage and concentrated electrolyte toward high energy density K-based dual-graphite battery, Adv. Energy. Mater. 10 (41) (2020) 2002567, https://doi.org/10.1002/aenm.202002567.

[29] A. Abouimrane, J. Ding, I.J. Davidson, Liquid electrolyte based on lithium bis-fluorosulfonyl imide salt: aluminum corrosion studies and lithium ion battery investigations, J. Power Sources 189 (1) (2009) 693–696, https://doi.org/10.1016/j.jpowsour.2008.08.077.

[30] G. Zhang, S. Wang, K. Ma, C. Wang, F. Zhou, X. Zhao, Z. Lv, Y. Zhang, High energy density potassium-based dual graphite battery with high concentration carbonate electrolyte, J. Pow. Sources 624 (2024) 235565, https://doi.org/10.1016/j.jpowsour.2024.235565.

[31] X.Y. Zhang, T.M. Devine, Factors that influence formation of AlF_3 passive film on aluminum in Li-ion battery electrolytes with $LiPF_6$, J. Electrochem. Soc. 153 (2006) B375–B383, https://doi.org/10.1149/1.2218816.

[32] T. Ma, G.-L. Xu, Y. Li, L. Wang, X. He, J. Zheng, J. Liu, M.H. Engelhard, P. Zapol, L. A. Curtiss, J. Jorne, K. Amine, Z. Chen, Revisiting the corrosion of the aluminum current collector in lithium-ion batteries, J. Phys. Chem. Lett. 8 (5) (2017) 1072–1077, https://doi.org/10.1021/acs.jpclett.6b02933.

[33] H. Tan, D. Zhai, F. Kang, B. Zhang, Synergistic PF_6^- and FSI^- intercalation enables stable graphite cathode for potassium-based dual ion battery, Carbon 178 (2021) 363–370, https://doi.org/10.1016/j.carbon.2021.03.027.

[34] G. Schmuelling, T. Placke, R. Kloepsch, O. Fromm, H.-W. Meyer, S. Passerini, M. Winter, X-ray diffraction studies of the electrochemical intercalation of bis (trifluoromethanesulfonyl)imide anions into graphite for dual-ion cells, J. Power Sources 239 (2013) 563–571, https://doi.org/10.1016/j.jpowsour.2013.03.064.

[35] J. Zheng, S. Myeong, W. Cho, P. Yan, J. Xiao, C. Wang, J. Cho, J.-G. Zhang, Mn-rich Li- and cathode materials: challenges to commercialization, Adv. Energy Mater. 7 (2017) 1601284, https://doi.org/10.1002/aenm.201601284.

[36] Sigma Aldrich Catalogue. https://www.sigmaaldrich.com/DE/de, 2025.

[37] M.V. Gorbunov, D. Mikhailova, Peculiarities in structural behaviour of graphite during anionic intercalation of PF_6^-, FSI^- and ClO_4^- at elevated temperature, Chem. Commun. 61 (2025) 5451–5454, https://doi.org/10.1039/D5CC00366K.

[38] N. Zhang, A. Eldesoky, R./.A. Dressler, J.R. Dahn, Surprising dependence of the exfoliation of graphite during formation on electrolyte composition, J. Electrochem. Soc. 170 (2023) 070517, https://doi.org/10.1149/1945-7111/ace65c.

[39] S.-I. Lee, U.-H. Jung, Y.-S. Kim, M.-H. Kim, D.-J. Ahn, H.-S. Chun, A study of electrochemical kinetics of lithium ion in organic electrolytes, Korean J. Chem. Eng. 19 (2002) 638, https://doi.org/10.1007/BF02699310.

[40] U. Tilsam, Sulfolane: a versatile dipolar aprotic solvent, Org. Process Res. Dev. 16 (7) (2012) 1273–1278, https://doi.org/10.1021/op300108w.

[41] Y. Ugata, Y. Chen, S. Sasagawa, K. Ueno, M. Watanabe, H. Mita, J. Shimura, M. Nagamine, K. Dokko, Eutectic electrolytes composed of $LiN(SO_2F)_2$ and sulfones for Li-ion batteries, J Phys. Chem. C 126 (24) (2022) 10024–10034, https://doi.org/10.1021/acs.jpcc.2c02922.

[42] Y. Ugata, Yichuan Chen, S. Miyazaki, S. Sasagawa, K. Ueno, M. Watanabe, K. Dokko, High-concentration LiPF6/sulfone electrolytes: structure, transport properties, and battery application, Phys. Chem. Chem. Phys. 25 (2023) 29566–29575, https://doi.org/10.1039/D3CP04561G.

[43] J. Jannelli, M.D. Monica, A. Della Monica, Gazz. Chim.Ital. 94 (1964) 552.

[44] U. Lamanna, O. Sciacovelli, L. Jannelli, ibid 96 (1966) 114.

[45] O.G. Reznitskikh, A.S. Istomina, S.S. Borisevich, E.Y. Evshchik, E.A. Sanginov, O. V. Bushkova, Y.A. Dobrovolsky, Phase diagram of ethylene carbonate–sulfolane system, Rus. J. Phys. Chem. A 95 (6) (2021) 1121–1127, https://doi.org/10.1134/S0036024421060224.

[46] L. Rycerz, Practical remarks concerning phase diagrams determination on the basis of differential scanning calorimetry measurements, J. Therm. Anal. Calorim. 113 (2013) 231, https://doi.org/10.1007/s10973-013-3097-0.

[47] Y. Lu, C.-Z. Zhao, H. Yuan, X.-B. Cheng, J.-Q. Huang, Q. Zhang, Critical current density in solid-State lithium metal batteries: mechanism, influences, and strategies, Adv. Funct. Mater. 31 (18) (2021) 2009925, https://doi.org/10.1002/adfm.202009925.

[48] W. Zhou, P.H.-L. Sit, First-principles understanding of the staging properties of the graphite intercalation compounds towards dual-ion battery applications, ACS Omega 5 (29) (2020) 18289–18300, https://doi.org/10.1021/acsomega.0c01950.

[49] M. Chugh, M. Jain, G. Wang, A. Shaygan Nia, H. Mirhosseini, T.D. Kühne, A combinatorial study of electrochemical anion intercalation into graphite, Mater. Res. Express 8 (2021) 085502, https://doi.org/10.1088/2053-1591/ac1965.

[50] J.A. Read, In-situ studies on the electrochemical intercalation of hexafluorophosphate anion in graphite with selective cointercalation of solvent, J. Phys. Chem. C 119 (2015) 8438–8446, https://doi.org/10.1021/jp5115465.

[51] M.S. Dresselhaus, G. Dresselhaus, Intercalation compounds of graphite, Adv. Phys. 51 (1) (2002) 1–186, https://doi.org/10.1080/00018730110113644.

[52] D. Zhu, L. Zhang, Y. Huang, J. Li, H. Fan, H. Wang, ACS Appl. Energ. Mater. 2 (2019) 8031–8038, https://doi.org/10.1021/acsaem.9b01508.

[53] V. Augustyn, J. Come, M.A. Lowe, J.W. Kim, P.-L. Taberna, S.H. Tolbert, H. D. Abruña, P. Simon, B. Dunn, High-rate electrochemical energy storage through Li^+ intercalation pseudocapacitance, Nat. Mat. 12 (2013) 518–522, https://doi.org/10.1038/nmat3601.

[54] J. Fischer, K. Thümmler, I. Zlotnikov, D. Mikhailova, S. Fischer, Synthesis of cellulose acetate butyrate microspheres as precursor for hard carbon-based electrodes in symmetric supercapacitors, Polymers 16 (2024) 2176, https://doi.org/10.3390/polym16152176.

[55] J. Asenbauer, T. Eisenmann, M. Kuenzel, A. Kazzazi, Z. Chen, D. Bresser, The success story of graphite as a lithium-ion anode material – fundamentals, remaining challenges, and recent developments including silicon (oxide) composites, Sustain. Energy Fuels 4 (2020) 5387–5416, https://doi.org/10.1039/D0SE00175A.